Compressor Stroke and Frequency Response Measurements Using Strain Gauges

H. Rana, P. Bailey, M. Dadd, R. Stone

Department of Engineering Science, University of Oxford
Oxford, OX1 3PJ

ABSTRACT

LVDTs are commonly used displacement transducer devices integrated into cryocooler compressors in order to measure displacement stroke. They present the particular drawback of phase lag in the measurement signal. When flexure springs in an Oxford-style cryocooler fail, the off-axis forces on the moving motor shaft will increase and lead to a compressor failure that will halt the operation of the cryocooler. It is therefore important that a suitable method for detecting cryocooler stroke be in place during operation in order to detect early signs of off-axis movement and potential failure.

The suitability of a novel method using strain gauges in a full Wheatstone bridge configuration, integrated onto a spring-moving magnet motor setup, is investigated in this study. Finite Element Analysis was conducted to explore regions of highest strain in the spring for a given displacement, which permitted appropriate strain gauge installation. The strain gauge bridge configuration was calibrated with an Omron laser displacement transducer and validated with the FEA model.

A variety of tests was then conducted on the system to understand its harmonic characteristics. Finally, a series of dynamic and impact tests was conducted, where measurements during continuous operation and during impact collisions of increasing force were investigated. An analysis of the strain gauge bridge signal output and phasor characteristics of the integrated setup was completed. This measurement technique was successful in measuring in-situ compressor stroke as well as demonstrating a strong frequency response with the ability to detect small impacts on the compressor amid operation.

INTRODUCTION

Cryocooler compressor stroke is measured using displacement transducer devices, where most commonly LVDTs are utilized [1] [2] [3]. These can often be subject to phase lag, however [4]. In this study, the suitability of a novel method using strain gauges in a full Wheatstone bridge configuration, integrated onto a spring and moving magnet motor setup, was investigated. FEA was used to assess regions of highest strain in the spring for a given displacement which then allowed the strain gauge to be located at the optimum location. A series of tests was completed to assess the suitability of the strain gauge bridge as a method of displacement measurement as well as ascertaining the frequency response to various modes of operation.

Cryocoolers 22, edited by R.G. Ross, Jr., J.R. Raab and S.D. Miller

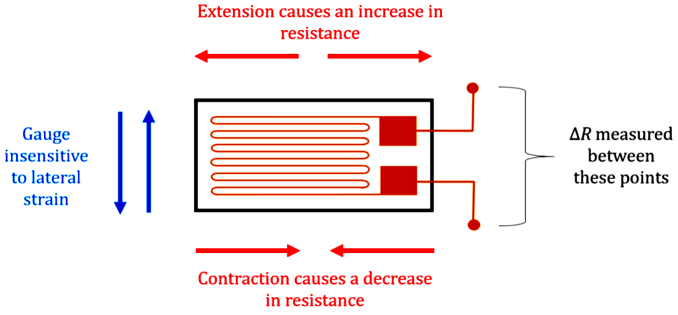

Figure 1. A single strain gauge bonded to a material surface is able to register changes in tension and compression to measure a change in strain.

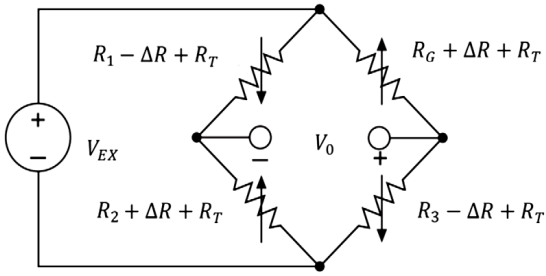

Figure 2. Full Wheatstone bridge configuration with four active strain gauges.

STRAIN GAUGE BRIDGE CIRCUIT

A single strain gauge bonded to a material surface is able to register changes in tension and compression as a change in strain. A schematic of a strain gauge is shown in Figure 1, where extension causes an increase in resistance and contraction results in a decrease in resistance. The difference in resistance can thus be measured across the gauge, which is insensitive to lateral strain. The unstressed strain gauge typically has a resistance, R_G, within the range of 30-3000 Ω [5] and a 0.1% strain leads to a change in resistance of approximately 0.2%. In order to measure small changes in resistance with higher accuracy, the strain gauges need to be in a bridge configuration.

The circuit configuration for four strain gauges in a full Wheatstone bridge is shown in Figure 2. This configuration balances out changes in resistance due to temperature (R_T); hence the circuit provides intrinsic temperature compensation. The output voltage, V_0, is given by Equation 1 below, where V_{EX} is the excitation voltage.

$$V_0 = V_{EX} [(R_3/(R_3 + R_G)) - (R_2/(R_1 + R_2))] \quad (1)$$

STRAIN GAUGE BRIDGE CIRCUIT

Finite Element Analysis

An FEA model of the spring arm was used to simulate the direction and magnitude of the principal stresses acting on the spring arm during displacement in the designed testing setup. A strain gauge was then installed onto each spring arm in the location and along the direction vector where the highest principal strain was observed in the simulation. Furthermore, the strain at the location of the installed strain gauge was computed for a range of spring arm displacements. Figure 3 shows a contour plot of strain along the spring arm along the *x*-axis, which is indicated by the coordinate system depicted. The coordinate system was defined with its origin at the location of the highest principal strain, and the *x*-axis was established along the vector direction of the highest principal strain. The origin therefore also represents where the strain gauge is to be installed.

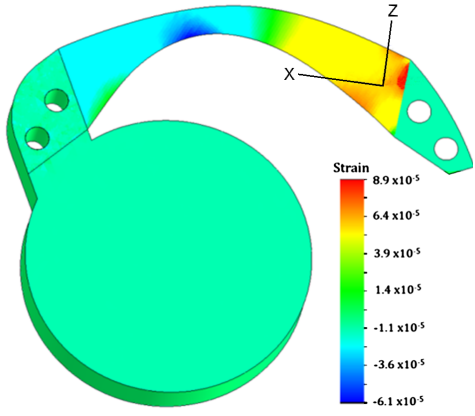

Figure 3. FEA contour plot strain along the spring arm.

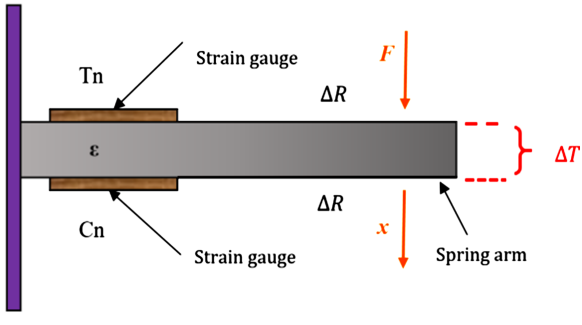

Figure 4. A strain gauge installed onto either side of the spring arm.

Strain Gauge Installation

The strain gauges are used in pairs per spring arm, where one will respond to compression and the other will register tension, by being mounted in parallel on either side of the spring arm surface. Any effect of temperature on the gauge resistance will therefore be cancelled. Figure 4 shows a schematic of the strain gauge pair installed on a single spring arm, where 'Tn', 'Cn', F, x and ΔT are tension, compression, force applied, spring arm displacement and change in temperature, respectively.

Testing Setup and FEA Validation

The testing setup used is shown in Figure 5. The strain gauges are installed in the full bridge configuration onto the spring assembly and an Omron laser displacement transducer is used to measure in-situ displacement. A moving magnet motor attached to the spring-strain gauge assembly is driven by an electromagnetic coil circuit. This testing rig is reported in further detail in 'Low cost flexure spring testing' [6]. The voltage output from the strain gauge full bridge is calibrated with the Omron-measured displacement to obtain a correlation for displacement.

The performance of the strain gauges in the experimental rig can be compared to that simulated in the FEA. Figure 6 shows the change in strain over a spring displacement range of ±8mm as simulated by the FEA compared with that obtained from the calibrated strain gauge bridge circuit. The discrepancy is observed given that the experimental strain gauge full bridge provides an output that is not a point measurement but an average over a larger area, whereas the FEA data is for a single point.

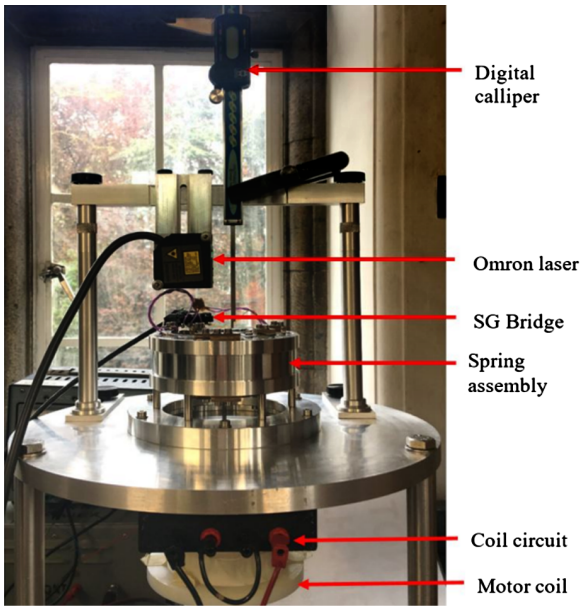

Figure 5. View of the strain gauge bridge testing setup where the strain gauge bridge is installed onto a spring assembly driven by a moving magnet motor.

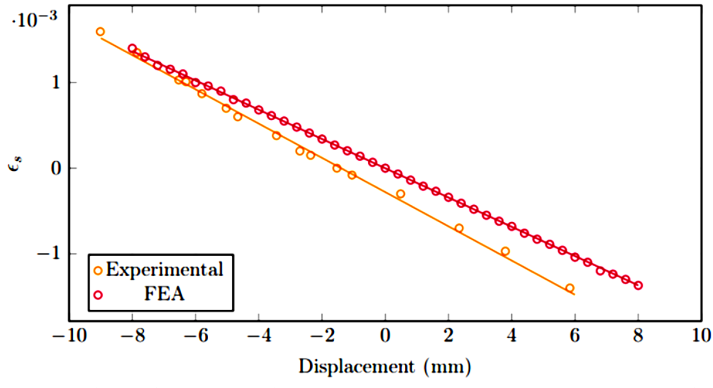

Figure 6. Change in strain as the spring over a ±8 mm range, as measured experimentally and as simulated in the FEA.

EXPERIMENTAL TESTING AND ANALYSIS

Dynamic Tests

The spring was oscillated at 15 Hz, its resonant frequency, while the spring displacement was incrementally increased. Figure 7 shows the two displacements calculated from the strain gauge and the Omron measurements, where both are in close agreement with an average error of 3.13%. The voltage output from the strain gauge full bridge is calibrated with the Omron-measured displacement to obtain a correlation for displacement.

Pluck Tests

A pluck force was applied to the spring to assess the frequency response of the strain gauge bridge. Figure 8 shows the signal output of the pluck test as registered by the strain gauge bridge, and Figure 9 shows the FFT plot of the output signal. A harmonic can be seen at approximately 4.3 kHz.

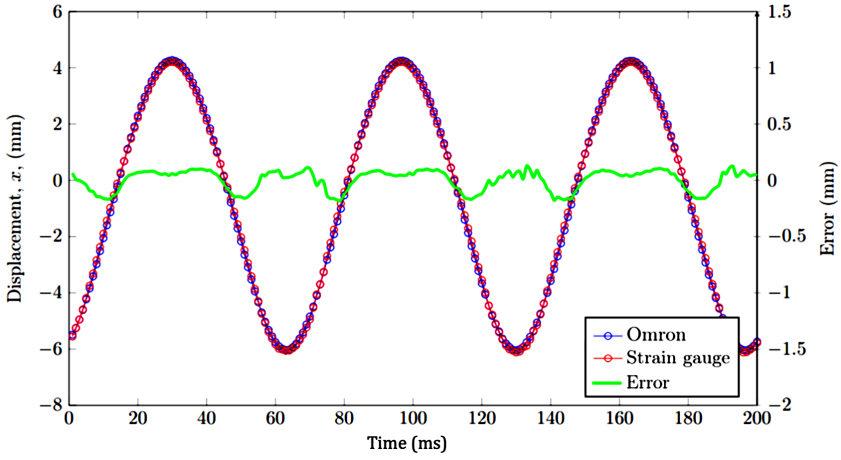

Figure 7. The output signals from the Omron transducer and the strain gauge bridge processed as armature stroke for 10 mm pk-pk amplitude. The difference between the two is displayed on the secondary axis.

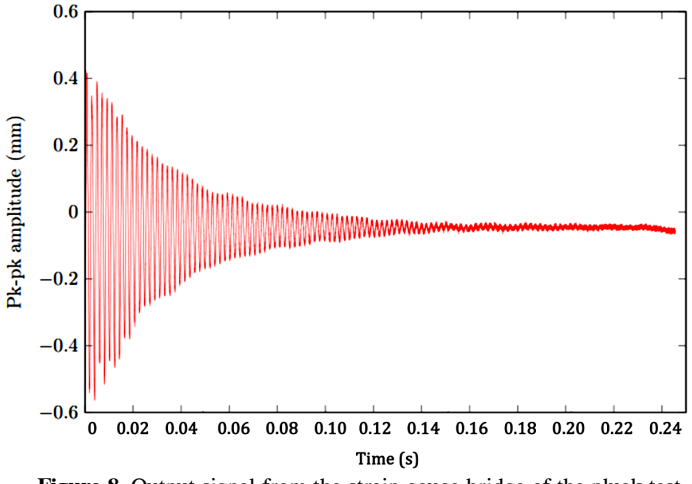

Figure 8. Output signal from the strain gauge bridge of the pluck test.

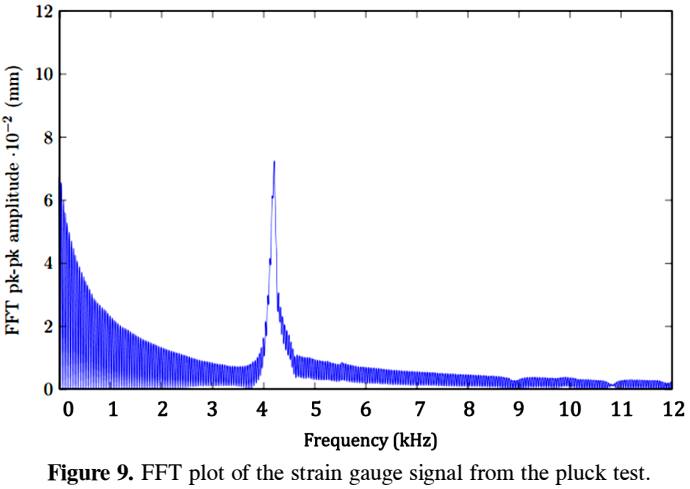

Figure 9. FFT plot of the strain gauge signal from the pluck test.

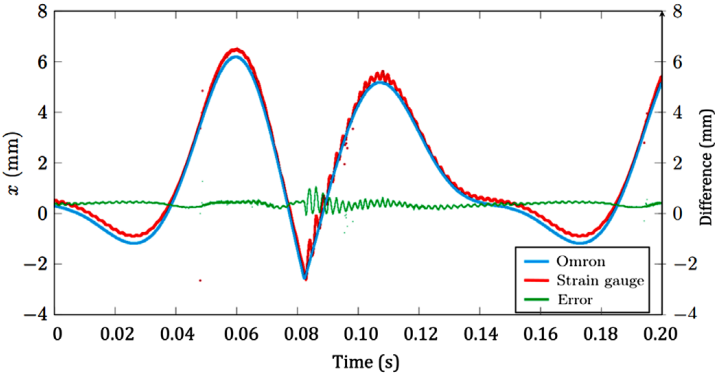

Figure 10. The computed output for displacement as measured by the strain gauge bridge and the Omron transducer during a fixed 4 mm impact and a stroke input of 11.5 mm and 14 Hz.

Impact Tests and Frequency Response

Fixed impact tests were completed by installing a fixed boundary at 4 mm distance above the spring which the spring arm would repeatedly hit whilst made to oscillate at varying amplitudes. The output signal for the strain gauge bridge and the Omron displacement is shown in Figure 10, where a drive voltage corresponding to a resultant spring stroke of 11.5 mm was supplied and fixed impact occurred at 4 mm. In the signal, sharpened motion can be seen in response to the impact, producing oscillations in the spring that the strain gauge bridge is able to detect. The difference in signals is due to vibrations of the spring arm, presumably at the natural frequency which was identified during the pluck test, which can be detected by the strain gauge bridge bonded directly to the spring arm. The Omron laser is likely correctly measuring the displacement at the centre of the setup but superimposed on this motion are the spring vibrations.

SUMMARY

The strain gauge bridge configuration was calibrated with an Omron laser displacement transducer and validated with the FEA model. A series of dynamic and impact tests was conducted, where measurement during continuous operation and during impact collisions of increasing force were investigated. This measurement technique was successful in measuring *in-situ* compressor stroke as well as demonstrating a strong frequency response with the ability to detect small impacts on the assembly amid operation.

ACKNOWLEDGEMENTS

The authors would like to acknowledge partial funding from the EPSRC with EP/N017013/1 and Honeywell Hymatic for this project and broader SPTC research within the Cryogenic Engineering group at the University of Oxford. Furthermore, the authors would like to thank the reviewers of *Cryocoolers*.

REFERENCES

1. Liang, K., “A review of linear compressors for refrigeration,” *International Journal of Refrigeration*, vol. 84 (2017).
2. Abolghasemi, M.A., et al., “Coaxial Stirling pulse tube cryocooler with active displacer,” *Cryogenics*, vol. 111 (2020).
3. Rana, H., et al., “A passive displacer for a Stirling pulse tube cryocooler,” *Cryocoolers 21*, ICC Press, Boulder, CO (2021), pp. 291-296.

4. Liang, K., et al., "Clearance seal compressors with linear motor drives. Part 2: Experimental evaluation of an oil-free compressor," *Proceedings of the Institution of Mechanical Engineers, Part: Journal of Power and Energy*, vol. 227 (2013).
5. Agilent Technologies, "Application notes 290-1: Practical strain gauge measurements," Tech. rep., RS Components UK (1999).
6. Bailey, P.B., et al., "Low cost flexure spring testing," *IOP Conference Series: Materials Science and Engineering*, vol. 502 (2019).